



ACCEPTED MANUSCRIPT

This is an early electronic version of an as-received manuscript that has been accepted for publication in the Journal of the Serbian Chemical Society but has not yet been subjected to the editing process and publishing procedure applied by the JSCS Editorial Office.

Please cite this article as T. T. H. Nguyen, N. T. Vu, H. M. Le, and H. S. Nguyen, *J. Serb. Chem. Soc.* (2025) <https://doi.org/10.2298/JSC241002005N>

This “raw” version of the manuscript is being provided to the authors and readers for their technical service. It must be stressed that the manuscript still has to be subjected to copyediting, typesetting, English grammar and syntax corrections, professional editing and authors’ review of the galley proof before it is published in its final form. Please note that during these publishing processes, many errors may emerge which could affect the final content of the manuscript and all legal disclaimers applied according to the policies of the Journal.



J. Serb. Chem. Soc. **00(0)** 1-13 (2025)
JSCS-13070

Effect of pyrolysis temperature and time of *Robusta* coffee husk on yield and product characteristics

THI THU HUONG NGUYEN*, NGOC TOAN VU, HONG MINH LE, HONG SON NGUYEN

Department of Chemical and Radiological Toxicology Technology Research, Institute of New Technology, Hanoi 122100, Vietnam.

(Received 2 October 2024; revised 10 October 2024; accepted 10 January 2025)

Abstract: The utilization and recycling of biochar from coffee husks is a global issue, as 1.8 million tons of coffee husks were produced in 2023. The mechanism of coffee husk pyrolysis and the factors influencing pyrolysis temperature and time on the properties of biochar were studied. Coffee husks were pyrolyzed at 350, 450, and 550 °C and held for 30, 45, 60 min to form biochar, the physicochemical properties of biochar were characterized by thermogravimetric analysis, X-ray diffraction, surface morphology, and Fourier-transform infrared spectroscopy. The pyrolysis of coffee husks occurs due to dehydration, decomposition, and carbonization reactions. Pyrolysis temperature and time directly affect the yield of biochar, pH, fixed carbon, volatile matter, ash, nitrogen, phosphorus, and potassium contents. Furthermore, pyrolysis temperature has a greater influence on the properties of biochar than pyrolysis time. The high potassium content of biochar can significantly replace conventional potash fertilizers. Therefore, biochar plays a dual role as a liming agent and can be used as a soil additive.

Keywords: pyrolysis mechanism; biochar properties; nitrogen content; phosphorus content; potassium content; soil additive.

INTRODUCTION

Over five billion tons of agricultural by-products are generated annually.¹ However, these agrarian by-product utilization options account for a small part because they are costly, laborious, and time-consuming.^{2,3} In the Central Highlands of Vietnam, agricultural by-products are often landfilled, stored on soil, and direct combustion after the end of the harvest season.⁴ These irreparable environmental effects, such as increased emissions of CH₄, N₂O, CO₂, loss of nutrients and soil fertility, and soil and groundwater pollution, affect human health and cause global warming.^{2,5} The conversion of agricultural by-products such as coffee husks into

* Corresponding author. E-mail: huong93mta@gmail.com
<https://doi.org/10.2298/JSC241002005N>

biochar as soil improvement additives provides nutrients to plants such as trace and macroelements, helps plants photosynthesize, and increases the sugar content of fruits.^{6,7,8} In addition, biochar is a carbon-rich material, which increases soil carbon storage, is biodegradable, some heavy metals convert to less toxic forms, eliminates pathogens, increases cation exchange capacity, increase pH, reduce compaction, and increase soil water holding capacity.^{2,9,10,11,12}

Biomass from agricultural, industrial, food, and forestry waste produces biochar.¹³ This biochar is produced by pyrolysis of biomass under temperature conditions from 350 °C to 600 °C and an oxygen-deficient environment.^{14,15} The products of the biomass pyrolysis process, in addition to biochar, also include bio-oil and gas.¹⁵ In 2023, Vietnamese coffee will be harvested at 29.2 million 60-kg bags, while world coffee will be 168.2 million 60-kg bags, meaning that Vietnamese coffee accounts for 17% of global production, and is the second largest coffee producer in the world.¹⁶ Since coffee husks account for about 18 % of the weight of fresh coffee cherries, more than 1.8 million tons of husks will be produced worldwide in 2023.^{17,18}

This by-product is currently less reused as a raw material for the biochar production process. Biochar characteristics depend on factors that affect the quantity and quality of charcoal production, namely temperature and pyrolysis time.¹⁹ Various studies have compared the efficiency of biochar generated at low and high temperatures for soil reclamation.^{20,21} However, the effects of coffee husk pyrolysis on temperature and time are still unclear. Furthermore, the pyrolysis mechanism of coffee husks has been little studied in previous studies due to the complex reactions and mechanisms.^{15,22} Determining the structure of biochar is also very important to clarify coal's physical and chemical properties.¹⁴

This research focuses on determining the biochar structure through TGA, XRD, FE-SEM and FTIR techniques and evaluating the physicochemical properties of biomass and biochar derived from coffee husks at different temperatures and pyrolysis times. Moreover, the mechanism of pyrolysis of coffee husks is also proposed.

EXPERIMENTAL

Reagents

o-Phenanthroline monohydrate ($C_{12}H_8N_2 \cdot H_2O$, ≥ 99.5 %, Merck, Germany). Sulfuric acid (H_2SO_4 , ≥ 95 %) and ethanol (C_2H_5OH , ≥ 99.8 %) from Fisher, UK. Nessler reagent, 2,4-dinitrophenol ($C_6H_4N_2O_5$, ≥ 99 %) from Alpha Chemika, India. Hydrochloric acid (HCl, 37 %), potassium dichromate ($K_2Cr_2O_7$, ≥ 99.8 %), phosphoric acid (H_3PO_4 , ≥ 85 %), nitric acid (HNO_3 concentrate, ≥ 65 %), iron (II) sulfate heptahydrate ($FeSO_4 \cdot 7H_2O$, ≥ 99 %), ammonium iron (II) sulfate hexahydrate ($FeSO_4(NH_4)_2SO_4 \cdot 6H_2O$, ≥ 99.5 %), sodium hydroxide (NaOH, ≥ 96 %), boric acid (H_3BO_3 , ≥ 99.5 %), methyl blue ($C_{37}H_{27}N_3Na_2O_9S_3$, ≥ 98.5 %), methyl red ($C_{15}H_{15}N_3O_2$, ≥ 95 %), ammonia solution (NH_4OH , 27 %) from Xilong, China. 0.1 mol/L HCl standard tube (Cemaco, Vietnam) and ultrapure water (Milli-Q Reference, Millipore, France).

Equipment

Analytical weighing (Shimadzu Auw220d, Japan), Drying cabinet (HN101, China), Sift (hole size 0.22 mm), Kiln (SX2-5-12, China), Ball mill (Retsch PM100, USA), pH measuring equipment (Mettler Toledo S220K, China), Distillation equipment UDK 139 (Velp, Italy), UV-Vis measuring equipment (Shimadzu 1900i, Japan), Flame photometer (FP6400, China).

TGA analysis using the Netzsch TG 209F1 Libra thermal analyzer (Netzsch Instrument Corp., Germany) in a nitrogen medium with a heating rate of 10 °C/min from a temperature of 30 °C to a final temperature of 800 °C with samples weighing about 5 mg to determine the thermal decomposition properties of coffee husks. Then, the first-order derivative of the TG function, the DTG curve, is used to determine the mass loss in the temperature range.

X-ray diffraction analysis is performed to detect all mineral phases and chemical structures present in biochar. Powdered biochar samples were fed into glass dishes and analyzed on the D8-Advance instrument (Bruker, Germany) with Cu K α radiation (wavelength about 1.5418 Å), measurement range 2 θ from 10° to 70°, with a jump of 0.03°. Mineral phases are determined by comparing and contrasting distances d with the ICDD standard database system.

The surface morphology of biochar samples was measured using a FE-SEM scanning electron microscope device (JSM-IT800, Japan). Samples were dried at 70 °C in an oven before SEM measurements.

Coffee husks, crushed biochar with KBr, pellets, then FTIR measurement on the Tensor II instrument (Bruker, Germany), wavelength range 400 to 4000 cm⁻¹, with a resolution of 1.4263 cm⁻¹ with 16 scans.

Raw material preparation and biochar production

Coffee husks of the Robusta variety (Fig. 1) are collected from households in Ea Tan commune, Krong Nang district, Dak Lak province. The sampling location is 13.10° N, 108.30° E, and transported to the experimental site, the Institute of New Technology. After being separated from the ripe coffee cherries, the coffee husks were dried on a tarpaulin for 5 days, avoiding direct sunlight. Then, the coffee husks were manually removed from impurities such as dry branches and filtered through a 3 mm sieve to remove soil. Oven-dried coffee husks were done at 70 °C for 8 hours. The samples were stored in sealed plastic containers at room temperature.

Biochar from seed husks is said to work well with soil when pyrolysis is at temperatures not more excellent than 550 °C, so this study selected temperatures of 350 °C, 450 °C, and 550 °C to conduct.²³ Nine types of biochar are produced from coffee husks with three pyrolysis temperatures (350, 450, and 550 °C) and pyrolysis time (30, 45, and 60 minutes). Before pyrolysis, coffee husks are dried at a temperature of 70 °C. In each pyrolysis process under an anoxygenic atmosphere, approximately 160 g of biomass mass was used. The final pyrolysis temperatures reached 350, 450, or 550 °C with a constant heating rate of 10 °C/min. The biochar samples were held for 30, 45, or 60 min at a final temperature, and then allowed to cool to room temperature. After that, the biochar samples are crushed by a ball mill for 1 hour at 300 rpm. After grinding the marbles, the samples are sieved through a 0.22 mm grid and dried at 70 °C for low humidity before analysis. The particle size of coffee husks is essential in the resulting biochar properties and affects the concentration of volatiles during pyrolysis.^{22,24} To address concerns related to particle size, the biochar in this study had a particle size no larger than 0.22 mm to increase uniformity in analysis.

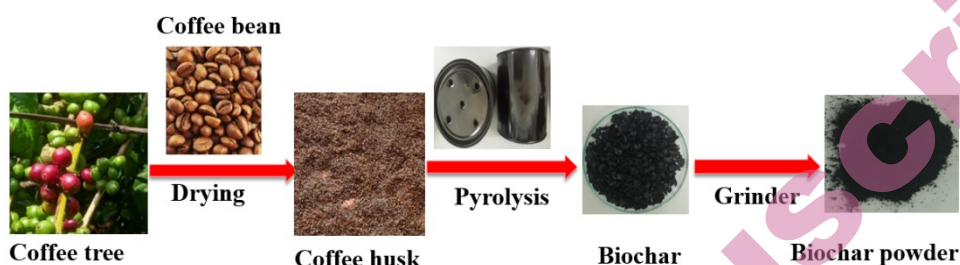


Fig. 1. The process of biochar formation

Characteristic assessment of properties of biochar

Biochar from coffee husks is characterized by pH, moisture content, performance, volatile solids content, ash, fixed carbon, calcification value, organic carbon, total nitrogen, phosphorus, and potassium.

The pH of biochar is determined according to ISO 10390:2021 by pH measuring equipment in water at 1:5 (v/v) immediately after shaking the sample for 1 h.

The moisture content of the biochar is obtained by drying about 5 g of the sample (recording the weighing mass before drying, m_0) in the drying cabinet at 70 °C to constant weight, and then weighing the mass after drying (m_s) to calculate the result according to the Equation (1).

$$\text{Humidity \%} = \frac{100(m_0 - m_s)}{m_0} \quad (1)$$

Volatile solids, ash, and fixed carbon are defined according to ASTM D1762-84 (2021). Biochar samples are placed in a covered crucible in a furnace at 950 °C for 6 minutes. Mass loss is associated with volatile material (DBH). That biochar is returned to the kiln at 750 °C for 6 hours. The material remaining after burning is ash. The fixed carbon content is determined by Equation (2).

$$\text{Fixed carbon (\%)} = 100 - \text{DBH} - \text{Ash} \quad (2)$$

The biochar calcification value is determined by acid-base titration using Equation (3).²⁵ Weigh 0.5 g of biochar and 20 mL of shake for 2 hours, then titrate with 0.1 mol/L HCl to the endpoint with pH = 2.0. To ensure that the pH of biochar is stable at 2.0 after 12 hours of equilibrium, the pH is measured again and adjusted with the above HCl solution if necessary. The volume of acid used and the pH value are recorded.

$$\text{Calcification value} = \text{total volume of HCl reaches stable value/pH range} \quad (3)$$

The total nitrogen content is determined by the Kjeldahl decomposition and distillation method in 3 stages: conversion of nitrogen compounds in the sample into ammonium by H₂SO₄ and catalyst (K₂SO₄ and Se) (stage 1), followed by distillation of ammonium by 40 % NaOH solution (stage 2), collect NH₃ (stage 3) with a solution of boric acid.²⁶ Stage 1: Weigh about 2 g of sample, add 1 g of catalyst (ratio of K₂SO₄ and Se to mass is 100:1), gradually increase the temperature to 200 °C, keep 200 °C for 120 minutes, continue to increase the temperature to 350 °C for about 60 min (until the white smoke is gone, the sample solution is clear), cool, add 50 mL of water, boil 10 minutes, add water until the volume of solution is 200 mL (solution A). Stage 2: Distillation of 30 mL of solution A using distillation equipment UDK 139 yields solution B. The installation mode of UDK 139 equipment is 50 mL H₂O, 50 mL NaOH 40 %, and 5 min. Solution B dissolves with 25 mL of 5 % boric acid. 25 mL of 5 % boric acid contains

0.5 mL of methyl blue-methyl-red color indicator. Ammonium was determined in the mixture using Nessler's reagent. The final stage: Titrate solution B with HCl 0.2 N. The nitrogen content is calculated by the Equation (4). In particular, V_{test} and V_0 are the volume of HCl 0.2 N used for titration of the test sample and the white sample (mL), and m is the mass of analyzed biochar (g).

$$N\% = \frac{0.2802(V_{test}-V_0)}{m} \quad (4)$$

The phosphorus content is determined by Equation (5) according to the molybdenum blue method measured by UV-Vis.²⁷ About 200 mL of 2 % citric acid solution contains 2 g of sample, shake for 60 minutes, filter through green tape filter paper, and obtain solution A. Take 20 mL of solution A, 1 mL H₂SO₄, 1 mL H₂O, boil slightly for about 30 minutes, add 10 mL of thick HNO₃, boil slightly until almost empty, cool, add 10 mL of water, boil 5 minutes, add water so that the volume reaches 50 mL (solution B). Measure optical absorption at a wavelength of 720 nm on a UV-Vis measuring device by preparing a solution before measuring as follows: The mixture has 5 mL of solution B, 5 mL of water, 2 drops of indicator α dinitrophenol, drip drops of 10 % NH₄OH until the solution turns yellow, then drip a few drops of 10 % HCl for all yellow, add 8 mL of molybdenum blue mixture, add water until the solution has a volume of 50 mL. Construct a calibration representing the correlation between photoadsorption and standard phosphorus solution concentration. Where Abs is the optical adsorption, m is the mass of analyzed biochar (g).

$$P\% = \frac{0.5(0.5114Abs-0.0054)}{m} \quad (5)$$

The potassium content is determined by a flame photometer with an extraction solvent of 0.05 N HCl.²⁸ The potassium content is calculated by the Equation (6). In particular, K_1 and K_0 are the potassium concentration in the sample and the white sample (mg/L), respectively, and m is the mass of biochar analyzed (g).

$$K\% = \frac{K_1-K_0}{42.768m} \quad (6)$$

Statistical analysis

The data is analyzed for variance analysis (ANOVA) to find significant differences between factors such as pyrolysis temperature, pyrolysis time, and their interaction. The test result reaches the F probability level of 0.05. All data is used using Origin (Software Origin, Version 9.85, OriginLab Corporation, Massachusetts, USA) for data analysis and graphing. The acronym T350-30 means that coffee husks are pyrolysis at 350 °C, and when it reaches 350 °C, they calcine for 30 minutes.

RESULTS AND DISCUSSION

Influence of pyrolysis temperature and time on biochar performance

The resulting biochar yield is calculated as the ratio between the volume of biochar obtained and biomass. The biochar yield decreased with increasing pyrolysis temperature (Fig. 2a). This is explained by the fact that as the temperature increases, moisture loss occurs, and large amounts of volatile organic compounds are released, resulting in a decrease in the volume of biochar formed.^{2,29} The 300-450 °C coal formation process produces an immense amount of coal biomass, consistent with the results of DTG spectroscopy and other research.³⁰ The increase

in pyrolysis time on the same low pyrolysis temperature (at 350 °C and 450 °C) also reduces the biochar yield (Fig. 2a) since the higher temperature leads to more cracking reactions occurring that change the internal structure and surface of biochar, similar to Hu and Das's reports.^{22,31}

Influence of pyrolysis temperature and time on the pH of biochar

The increased pyrolysis temperature and time cause the pH of biochar to increase. Overall, the pH value of biochar is higher than 9 (Fig. 2b). This is explained by the relative concentration of non-pyrolyzed inorganic elements already present in the original coffee husk, the cations in the ash are enriched, the loss of acid functional groups, and the formation of oxides, hydroxides, alkalis such as Ca-Mg-bearing K, Na-, carbonate mineral phases and reduced concentration of functional groups on acidic surfaces.^{8,31,32} Compared to the pH of coffee husks (pH = 6.5), pyrolysis increases the pH in water, and the pH value increases to 3.5 units of biomass when pyrolysis is at 550 °C (Fig. 2b). The pH value of biochar increases with increasing pyrolysis temperature, which has been reported with biochar from rice straw and sawdust.^{19,33} Among biochar, the highest pH value was recorded in pyrolysis coffee husks at 550 °C for 60 minutes, and pH was 10.1.

To produce biochar with pH = 10, a 57 % increase in pyrolysis temperature (from 350 to 550 °C) is necessary. However, doubling the time (from 30 to 60 minutes) at the same pyrolysis temperature of 350 or 450 °C) still cannot produce biochar with a pH of around 10. This shows that the pyrolysis temperature has a more significant influence on the pH of biochar than the pyrolysis time.

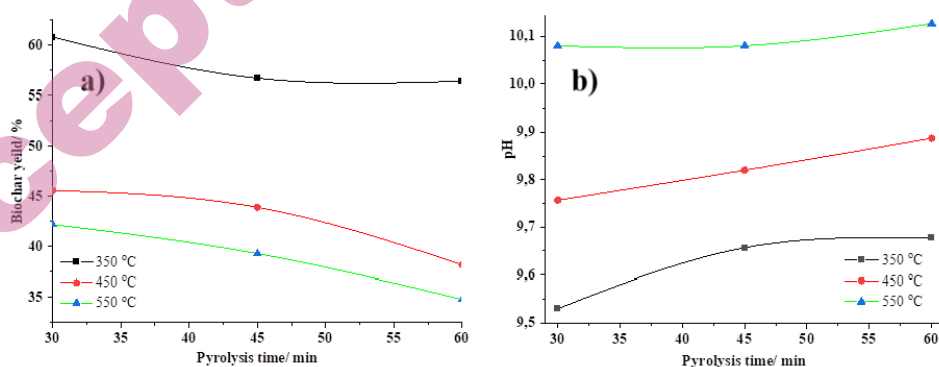


Fig. 2. (a) Biochar performance is obtained at different temperatures and pyrolysis times; (b) pH of biochar at different temperatures and pyrolysis times

Influence of pyrolysis temperature and time on the content of elements (N, P, K) of biochar

The pyrolysis temperature and time values of coffee husks are directly proportional to the content of phosphorus, and potassium and inversely proportional to the nitrogen content of biochar (Fig. S1). Sometimes, the

temperature and duration of pyrolysis increases, and the nitrogen content decreases. This result is consistent with the research of Das and Pariyar.^{2,14} This is explained by the volatility of nitrogen during pyrolysis, which causes nitrogen loss.¹⁴ When using biochar to fertilize crops, additional fertilizers, especially nitrogen, should be applied to avoid nitrogen fixation in the soil and maintain soil fertility. However, N fixation can be a beneficial mechanism to minimize N₂O emissions and reduce the amount of N leached from soil.³⁴ Notably, all types of biochar contain significant amounts of phosphorus (Fig. S1). This may be due to the interaction process between organic compounds and PO₄³⁻, producing a precipitate of phosphorus oxide.² The high potassium content in coffee husks (Fig. S1) can significantly replace the conventional source K, which serves as a slow-release fertilizer K, indicating these biochars' high agronomic value.¹² The high K content in biochar (Fig. S1) is mainly because carbonates and oxides of K are more soluble in water than carbonates and oxides of Mg and Ca.² Biochar pyrolysis occurs at low temperatures and takes less time, and nutrients such as K and P dissolve in acid lower.² Nitrogen, phosphorus, and potassium help biochar play a role in adding minerals to soil and plants.

Influence of temperature and pyrolysis time on the physical properties of biochar

The higher the temperature and pyrolysis time of coffee husks, the higher the fixed carbon and ash content while reducing biochar's volatile content (Fig. S2). In addition, Fig. S2 shows high fixed carbon content in biochar samples (85.67 %) and high volatile matter content in coffee husk samples (80.66 %). Coffee husks and biochar have different moisture contents.

Fig. S2 shows apparent differences in ash content between biochar samples. The ash content in biochar ranges from 12.68 to 22.51 %. The high ash content in biochar from coffee husks can be attributed to the high content of K (4.29 %) in biomass (Fig. S2) to protect the composition of organic substances and the structure of biochar during pyrolysis.³⁵ High ash content is associated with KHCO₃, verified by XRD analysis (Fig. S2). The fixed carbon content is inversely proportional to the ash content (Fig. S2). However, all are below 9 % (Fig. S2), sufficient for determining the content of volatiles, ash, and fixed carbon.³⁶ The moisture content in the samples can be thought to be the free water content, the amount of desiccant water present in the cell wall, and linked to hydroxyl groups.¹⁴ That characteristic makes biochar from coffee husks a potential material to increase the acidity neutralization ability of the soil to overcome the acidity of the soil.

Coffee husks have a high volatile matter content (80.66 %), which makes pyrolysis occur faster (Fig. S2), similar to Yousef's report when studying mangoes.³⁶ The volatile content of biochar decreases when the pyrolysis temperature increases from 450 °C to 550 °C (Fig. S2). This is explained by the increase in aromatization, water evaporation, low molecular weight hydrocarbons

and increased hydroxide and carbonate content, the presence of lignin that can resist thermal decomposition at temperatures of 450 °C, but not at temperatures as high as 550 °C.³⁷ The magnitude of the volatile matter content in biochar is a vital attribute for evaluating the C and N-cycle bioavailability of biochar in the soil ecosystem.

The ability to neutralize acidity was assessed through the reduced calcification value of biochar with increasing temperature and pyrolysis time of coffee husks (Fig. 3c). That said, soil acidity is judged by calcification value and pH. In addition, at any temperature, the pyrolysis of coffee husks has a higher calcification value than other types of biochar, which is related to the high concentration of minerals present in biochar, especially KHCO₃ found in XRD spectroscopy (Fig. S2).³⁸ Therefore, the calcification value of biochar is mainly adjusted by the ash content of coal, chemical composition (especially basic cations), and pH of biochar. This characteristic should be considered when applying biochar to the soil to adjust soil acidity.

Spectral characteristics

The TGA technique has been used to determine coffee husks' decomposition temperature and evaluate coffee husks' kinetics and other reactions over a wide temperature range of 0-800 °C (Fig. 3b). The TG curve clearly shows these phases (Fig. 3b, black). The DTG curve of coffee husks is used to determine the main composition of biomass during thermal decomposition (Fig. 3b, red).

The thermal decomposition process of coffee husks is divided into three main stages: dehydration, decomposition, and coalization. The dehydration stage and low weight volatiles from room temperature to 190 °C. Water evaporation causes disruption of bonds and the formation of hydroperoxide groups, -COOH and -CO.²² The initial 6.92 % weight loss was attributed to the moisture content of the coffee husk sample, as noted rice husk.³⁹ The stage of decomposition of hemicellulose, cellulose, and a small fraction of high lignin is from 190 °C to 450 °C, forming into biochar, bio-oil, and gas. The most prominent degradation peak of coffee husks is 307.3 °C. Coffee husks cannot be used for synthetic applications as they are high thermal strength material, and they will decompose when the processing temperature is more significant than 190 °C. This situation is common in food waste such as mango peels, bagasse, bean husks, and corn stalks.^{15,36} Above 450 °C, thermal decomposition occurs more slowly due to the slow decomposition of lignin and carbon-containing solids. The heating rate increases, resulting in a shift of the TG curve to a temperature of 800 °C due to better heat transfer to the inside of the coffee husk. Fig. 3b shows that hemicellulose, cellulose, and lignin have decomposition temperature ranges corresponding to 3 characteristic peaks at 204 °C, 307 °C, and 529 °C, consistent with the Chin-Pampillo report.²² In summary, the thermal decomposition mechanism is necessary to determine the change in biochar's physicochemical properties and its application.

XRD of biochar samples from coffee husks at different temperatures and pyrolysis times to determine the mineral composition in crystalline form in biochar

(Fig. 3c). Peaks at $2\theta = 40.6445^\circ$ are thought to be the presence of KCl. The presence of SiO_2 is also found from peaks at $2\theta = 49.2262^\circ$; 60.6585° in XRD spectrum. The peak of SiO_2 is more substantial at the pyrolysis husk at 450-550 °C and for 45-60 minutes (Fig. 3c). Biochar at three pyrolysis temperatures containing KHCO_3 , SiO_2 , and KCl was also observed report on weeds and on rice straw.^{2,3} The sharpness and peak intensity of the peaks increased slightly as the temperature and pyrolysis time increased, indicating that the crystalline mineral content evenly increased in biochar. Pyrolysis temperatures above 450 °C and pyrolysis times above 45 minutes appear stronger peaks, indicating that part of the cellulose's crystal structure has been lost, similar to a different report.⁴⁰ Peak magnitude at $2\theta = 24.1345^\circ$; 29.8655° ; 31.1424° shows the relative accumulation of KHCO_3 in biochar from coffee husks (Fig. 3c). The formation of KHCO_3 is facilitated by the reaction of K and CO_2 released during the thermal decomposition of hemicellulose and cellulose. The increased KHCO_3 content can also be explained by the high carbon content in coffee husks' biochar.

FE-SEM results show that coffee husks and biochar have rough surfaces and most of them have irregular shapes (Fig. 3a). The more you increase the pyrolysis temperature and the pyrolysis time, the biochar surface becomes smoother, the number of pores increases, the pore size increases and has a somewhat honeycomb-like structure, so the biochar has greater porosity (Fig. 3a). At a pyrolysis temperature of 450 °C and a pyrolysis time of 60 minutes, biochar has a more porous structure, rougher surface, and larger pore size. The pores on the biochar surface help microorganisms grow and the porosity of biochar helps increase water retention.⁴¹ This is explained by the evaporation of water and volatile substances.⁴²

FTIR spectroscopy of biomass and biochar obtained at different temperatures and pyrolysis times is shown in Fig. 3d. Table S1 presents the characteristics of the functional groups. Fig. 3d shows the peak characteristics of coffee husks' firm, medium, and weak decomposition before and after pyrolysis at 350, 450, and 550 °C for 30, 45, and 60 minutes. With increasing temperature and pyrolysis time, the base content of the functional group in the aromatic ring increases, while the content of acid-containing groups (-OH of phenol and C=O) decreases. Organic groups exist, even at high pyrolysis temperatures and long pyrolysis times, which may be associated with high ash content. Ash acts as a heat-resistant component, which can protect organic compounds against decomposition and hinder the formation of aromatic compounds as the temperature and pyrolysis time increase.²⁵

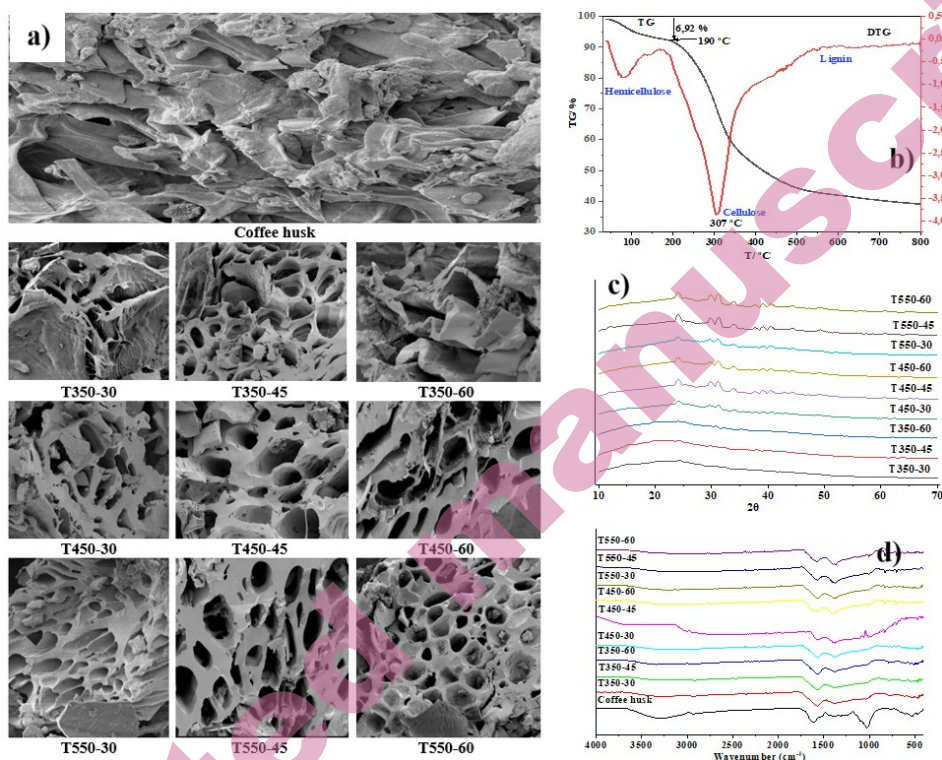


Fig. 3. (a) FE-SEM of biochar samples (3000x magnification); (b) Thermal analysis TG (black line) and DTG (red line) of coffee husks; (c) XRD patterns of biochar; (d) FTIR spectrum of coffee husks and biochar types from coffee husks at different temperatures and times

CONCLUSION

Robusta coffee husks are the raw materials used to make 9 types of biochar, using temperature and pyrolysis time control processes. Increasing temperature and pyrolysis time reduce biochar generation performance, volatiles, surface functional groups, nitrogen content, and increased pH, ash content, fixed carbon, organic carbon, phosphorus, and potassium. Moreover, the pyrolysis temperature dramatically affects the pyrolysis time on the above characteristics of biochar. Biochars are characterized by high calcification value, which makes them a potential material for regulating soil acidity. This biochar serves as a source of P and K for plants. The more the temperature and pyrolysis time increase, the more stable and precise the phase structure of KHCO_3 . With increasing temperature and pyrolysis time, the base content of the functional group in the aromatic ring increases, while the content of acid-containing groups ($-\text{OH}$ of phenol and $\text{C}=\text{O}$) decreases. Thus, biochar plays a dual role as a liming agent and a source of

nutrients for the soil to grow crops. Biochar is made at 450 °C for 60 minutes for the best, energy-saving, and environmentally friendly nutritional content.

SUPPLEMENTARY MATERIAL

Additional data are available electronically at the pages of journal website: <https://www.shd-pub.org.rs/index.php/JSCS/article/view/13070>, or from the corresponding author on request.

Acknowledgements: The authors thank the financial support of the science and technology project at the Ministry of Natural Resources and Environment to complete this work.

ИЗВОД

УТИЦАЈ ТЕМПЕРАТУРЕ И ВРЕМЕНА ПИРОЛИЗЕ ЉУСКЕ КАФЕ РОБУСТА НА ПРИНОС И КАРАКТЕРИСТИКЕ ПРОИЗВОДА

THI THU HUONG NGUYEN, NGOC TOAN VU, HONG MINH LE, HONG SON NGUYEN

¹Пољопривредни факултет, Универзитет у Београду, Немањина 6, Земун, Србија, ²Хемијски факултет, Универзитет у Београду, Студентски центар 12-16, Београд, Србија, ³Institute for Geology and Geochemistry of Petroleum and Coal, RWTH, Lochnerstr. 4-20, Aachen, Germany, ⁴Факултет за физичку хемију, Универзитет у Београду, Студентски центар 12-16, Београд, Србија и ⁵Институт за хемију, технологију и металургију, Национални институт Републике Србије, Његошева 12, Београд, Србија.

Коришћење и рециклажа биоугља из љуски кафе је глобално питање, с обзиром да је 2023. године произведено 1,8 милиона тона љуски кафе. Проучавани су механизам пироллизе љуске кафе и фактори као што су температура и време пироллизе који утичу на својства биоугља. Љуске од кафе су пиролизоване на 350, 450 и 550 °C и држане 30, 45, 60 минута на дајој температури, да би се формирао биоугаљ, а физичко-хемијска својства биоугља су окарактерисана термогравиметријском анализом, рендгенском дифракцијом, испитивањем морфологије површине и инфрацрвеном спектроскопијом са Фуријеовом трансформацијом. Пироллиза љуски кафе настаје услед реакција дехидрације, разлагања и карбонизације. Температура и време пироллизе директно утичу на принос биоугља, рН, фиксни угљеник, испарљиве материје, пепео, азот, фосфор и садржај калијума. Осим тога, температура пироллизе има већи утицај на својства биоугља него време пироллизе. Висок садржај калијума у биоугљу може у великој мери да служи као замена за конвенционална калијумова ђубрива. Због тога, биоугаљ игра двоструку улогу као „limiting“ агенс, и може се користити као додаток земљишту.

(Примљено 2. октобра 2024; ревидирано 10. октобра 2024; прихваћено 10. јануара 2025.)

REFERENCES

1. R. Shinde, D. K. Shahi, P. Mahapatra, C. S. Singh, S. K. Naik, N. Thombare, A. K. Singh, *Ind. Crops Prod.* **181** (2022) 114772 (<https://doi.org/10.1016/j.indcrop.2022.114772>)
2. S. K. Das, G. K. Ghosh, R. Avasthe, K. Sinha, *J. Hazard. Mater.* **407** (2021) 124370 (<https://doi.org/10.1016/j.jhazmat.2020.124370>)
3. A. S. El-Hassanin, M. R. Samak, S. R. Radwan, G. A. El-Chaghaby, *Environ. Nat. Resour. J.* **18** (2020) 283 (<https://doi.org/10.32526/enrj.18.3.2020.27>)

4. E. Cassou, S. M. Jaffee, J. Ru, *The challenge of agricultural pollution: evidence from China, Vietnam, and the Philippines*, World Bank Publications, 2018
5. N. Kumar, A. Chaudhary, O. Ahlawat, A. Naorem, G. Upadhyay, R. Chhokar, S. Gill, A. Khippal, S. Tripathi, G. Singh, *Soil Till. Res.* **228** (2023) 105641 (<https://doi.org/10.1016/j.still.2023.105641>)
6. C. Doulgeris, Z. Kyritidou, V. Kinigopoulou, E. Hatzigiannakis, *J. Agron.* **13** (2023) 784 (<https://doi.org/10.3390/agronomy13030784>)
7. G. Enaime, M. Lübken, *Appl. Sci.* **11** (2021) 8914 (<https://doi.org/10.3390/app11198914>)
8. Z. Elkhilifi, J. Iftikhar, M. Sarraf, B. Ali, M. H. Saleem, I. Ibranshahib, M. D. Bispo, L. Meili, S. Ercisli, E. Torun Kayabasi, *Sustainability* **15** (2023) 2527 (<https://doi.org/10.3390/su15032527>)
9. M. Irfan, M. Mudassir, M. J. Khan, K. M. Dawar, D. Muhammad, I. A. Mian, W. Ali, S. Fahad, S. Saud, Z. Hayat, *Sci. Rep.* **11** (2021) 18416 (<https://doi.org/10.1038/s41598-021-97525-8>)
10. Z. Liu, Z. Xu, L. Xu, F. Buyong, T. C. Chay, Z. Li, Y. Cai, B. Hu, Y. Zhu, X. Wang, *Carbon Res.* **1** (2022) 8 (<https://doi.org/10.1007/s44246-022-00007-3>)
11. J. Poveda, Á. Martínez-Gómez, C. Fenoll, C. Escobar, *Phytopathology*® **111** (2021) 1490 (<https://doi.org/10.1094/PHTO-06-20-0248-RVW>)
12. M. Z. Hossain, M. M. Bahar, B. Sarkar, S. W. Donne, Y. S. Ok, K. N. Palansooriya, M. B. Kirkham, S. Chowdhury, N. Bolan, *Biochar* **2** (2020) 379 (<https://doi.org/10.1007/s42773-020-00065-z>)
13. M. Antar, D. Lyu, M. Nazari, A. Shah, X. Zhou, D. L. Smith, *Renew. Sustain. Energy Rev.* **139** (2021) 110691 (<https://doi.org/10.1016/j.rser.2020.110691>)
14. P. Pariyar, K. Kumari, M. K. Jain, P. S. Jadhao, *Sci. Total Environ.* **713** (2020) 136433 (<https://doi.org/10.1016/j.scitotenv.2019.136433>)
15. J. E. Silva, G. Q. Calixto, C. C. de Almeida, D. M. Melo, M. A. Melo, J. C. Freitas, R. M. Braga, *J. Therm. Anal. Calorim.* **137** (2019) 1635 (<https://doi.org/10.1007/s10973-019-08048-4>)
16. G. M. Ngure, K. N. Watanabe, *Front. Sustain. Food Syst.* **8** (2024) (<https://doi.org/10.3389/fsufs.2024.1431849>)
17. R. Manrique, D. Vásquez, C. Ceballos, F. Chejne, A. s. Amell, *ACS Omega* **4** (2019) 2957 (<https://doi.org/10.1021/acsomega.8b02591>)
18. N. T. H. Thăng, *Eur. J. Bus. Res.* **7** (2022) (<https://doi.org/10.24018/ejbmr.2022.7.3.1356>)
19. S. Chandra, J. Bhattacharya, *J. Clean. Prod.* **215** (2019) 1123 (<https://doi.org/10.1016/j.jclepro.2019.01.079>)
20. C. Setter, F. Silva, M. Assis, C. Ataíde, P. Trugilho, T. Oliveira, *Fuel* **261** (2020) 116420 (<https://doi.org/10.1016/j.fuel.2019.116420>)
21. J. S. Chin-Pampillo, A. Alfaro-Vargas, R. Rojas, C. E. Giacomelli, M. Perez-Villanueva, C. Chinchilla-Soto, J. M. Alcañiz, X. Domene, *Biomass Convers. Biorefin.* **11** (2021) 1775 (<https://doi.org/10.1007/s13399-020-00714-0>)
22. X. Hu, M. Gholizadeh, *J. Energy Chem.* **39** (2019) 109 (<https://doi.org/10.1016/j.jechem.2019.01.024>)
23. N. Panwar, A. Pawar, B. Salvi, *SN Appl. Sci.* **1** (2019) 1 (<https://doi.org/10.1007/s42452-019-0172-6>)

24. B. Deng, X. Yuan, E. Siemann, S. Wang, H. Fang, B. Wang, Y. Gao, N. Shad, X. Liu, W. Zhang, *J. Waste Manag.* **120** (2021) 33 (<https://doi.org/10.1016/j.wasman.2020.11.015>)
25. R. R. Domingues, P. F. Trugilho, C. A. Silva, I. C. N. d. Melo, L. C. Melo, Z. M. Magriotis, M. A. Sánchez-Monedero, *PLoS one* **12** (2017) e0176884 (<https://doi.org/10.1371/journal.pone.0176884>)
26. S. Khajavi-Shojaei, A. Moezzi, M. Norouzi Masir, M. Taghavi, *Biomass Conv. Bioref.* **13** (2023) 593 (<https://doi.org/10.1007/s13399-020-01137-7>)
27. Y. Li, D. Xu, Y. Guan, K. Yu, W. Wang, *Int. J. Phytoremediation* **21** (2019) 145 (<https://doi.org/10.1080/15226514.2018.1488806>)
28. A. T. Nguyen, T. A. Bui, N. T. Mai, H. T. Tran, S. V. Tran, N. H. Nguyen, T. Tsubota, Y. Shinogi, S. Dultz, M. N. Nguyen, *J. Agron.* **112** (2020) 1713 (<https://doi.org/10.1002/agj2.20209>)
29. A. Tomczyk, Z. Sokółowska, P. Boguta, *Rev. Environ. Sci. Biotechnol.* **19** (2020) 191 (<https://doi.org/10.1007/s11157-020-09523-3>)
30. D. F. d. O. Torchia, E. Zonta, A. M. de Andrade, A. C. García, *Braz. J. Chem. Eng.* **39** (2022) 415 (<https://doi.org/10.1007/s43153-021-00147-w>)
31. S. K. Das, G. K. Ghosh, R. Avasthe, K. Sinha, *J. Environ. Manage.* **278** (2021) 111501 (<https://doi.org/10.1016/j.jenvman.2020.111501>)
32. S. Yu, W. Zhang, X. Dong, F. Wang, W. Yang, C. Liu, D. Chen, *J. Environ. Chem. Eng.* (2023) 111638 (<https://doi.org/10.1016/j.jece.2023.111638>)
33. D. Xu, J. Cao, Y. Li, A. Howard, K. Yu, *Waste Manag.* **87** (2019) 652 (<https://doi.org/10.1016/j.wasman.2019.02.049>)
34. Q. Liu, B. Liu, Y. Zhang, T. Hu, Z. Lin, G. Liu, X. Wang, J. Ma, H. Wang, H. Jin, *Global Change Biology* **25** (2019) 2077 (<https://doi.org/10.1111/gcb.14613>)
35. M. M. Afessa, P. Debiagi, A. I. Ferreira, M. A. Mendes, T. Faravelli, A. V. Ramayya, *J. Anal. Appl. Pyrol.* **162** (2022) 105435 (<https://doi.org/10.1016/j.jaap.2022.105435>)
36. S. Yousef, J. Eimontas, N. Striūgas, M. A. Abdelnaby, *Renew. Energy* **173** (2021) 733 (<https://doi.org/10.1016/j.renene.2021.04.034>)
37. T. Wang, H. Liu, C. Duan, R. Xu, Z. Zhang, D. She, J. Zheng, *Materials* **13** (2020) 3391 (<https://doi.org/10.3390/ma13153391>)
38. A. Bayata, G. Mulatu, *Am. J. Chem. Eng.* **13** (2024) 13 (<https://doi.org/10.11648/j.ajche.20241202.11>)
39. Z. R. Gajera, K. Verma, S. P. Tekade, A. N. Sawarkar, *Bioresour. Technol. Rep.* **11** (2020) 100479 (<https://doi.org/10.1016/j.biteb.2020.100479>)
40. B. C. Chaves Fernandes, K. Ferreira Mendes, A. F. Dias Júnior, V. P. da Silva Caldeira, T. M. da Silva Teófilo, T. Severo Silva, V. Mendonça, M. de Freitas Souza, D. Valadão Silva, *Materials* **13** (2020) 5841 (<https://doi.org/10.3390/ma13245841>)
41. J. W. Wong, U. O. Ogbonnaya, *Environ. Sci. Pollut. Res.* **28** (2021) (<https://doi.org/10.1007/s11356-021-14803-8>)
42. N.-T. Vu, K.-U. Do, *Biomass Conv. Bioref.* **13** (2023) 2193 (<https://doi.org/10.1007/s13399-021-01337-9>).